Seismocardiographic Signal Variability During Regular Breathing and Breath Hold in Healthy Adults

Md Khurshidul Azad[1],Peshala T Gamage[1], Richard H. Sandler[1,2], Nirav Raval[3], Hansen A. Mansy[1,2]
1. Biomedical Acoustic Research Lab, University of Central Florida, Orlando, FL 32816, USA
2. Biomedical Acoustic Research Company, Orlando, FL32812, USA,
3. Advent Health, Orlando, FL32803, USA
{khurshid@knights,peshala@knights., hansen.mansy@} ucf.edu , rhsandler@gmail.com

Abstract— Seismocardiographic signals (SCG) are known to correlate with mechanical cardiac activity and may be used for monitoring patients with cardiovascular disease. However, SCG variability is not well understood and may interfere with signal utility. In the current study, the SCG signals were acquired in 5 healthy subjects during regular breathing along with ECG and respiratory flow measurements. In addition, SCG waveforms were recorded during breath hold at end inspiration as well as end expiration. The SCG events were identified and segmented using ECG events. SCG waveforms during regular breathing were separated into two clusters using unsupervised machine learning. The variability was assessed for the clustered and un-clustered SCG by analyzing the Dynamic Time Warping (DTW) distances of SCG waveforms in the time domain. The inter-group variability between the normal breathing clusters and breath hold suggested that cluster 2 events were more similar to end expiration events while no clear trend was observed for cluster 1. The intra-group variability was reduced by approximately 19% for regular breathing clusters and 42% during breath hold compared to the un-clustered SCG during normal breathing. The reduced variability during breath hold suggests the utility of SCG recording at breath hold since variability reduction can lead to more robust methods for longitudinal patient monitoring.

Keywords- Seismocardiogrphy, variability, dissimilarity, monitoring, respiratory effect.

I. INTRODUCTION

Seismocardiographic (SCG) signals are chest wall vibrations due to cardiac activity[1]. Early studies [2]–[7] suggested that the mechanical processes involved in cardiac activity such as valve closures, blood momentum changes, cardiac muscle contraction are likely sources of these vibrations. SCG signals may provide useful information regarding cardiac function and, therefore, may be helpful in the diagnosis and monitoring of cardiovascular conditions. Some studies [8]–[10] extracted different cardiac parameters such as heart rate or systolic time intervals from SCG signals. Other studies[11]–[13] extracted respiratory information from the SCG signals.

SCG is typically measured over the chest surface (rather than directly on the heart) and respiration is known to cause morphological variabilities in SCG signal. This may be due to the change in heart shape and positioning, along with variations in intrathoracic pressure (i.e. pressure around the heart) during respiration. These variabilities may mask important SCG morphological features with diagnostic value, or conversely, may introduce errors in SCG interpretation. Hence, SCG potential utility should be improved by decreasing variability and/or enhancing our understanding of variability sources. The latter may help both account for SCG variability, but also serve as useful features to help improve the diagnostic predictive value.

Previous studies [9], [14] used respiratory information to group SCG events into their respiratory phases (respiratory flow or lung volume phases) to help reduce this variability. However, a recent study [15] suggested that SCG waveforms were better grouped using unsupervised machine learning based on minimum intra-group heterogeneity. This appears to stem from an observation that SCG event grouping based on lung volume phases may yield more homogeneous data than that based on respiratory flow phase.

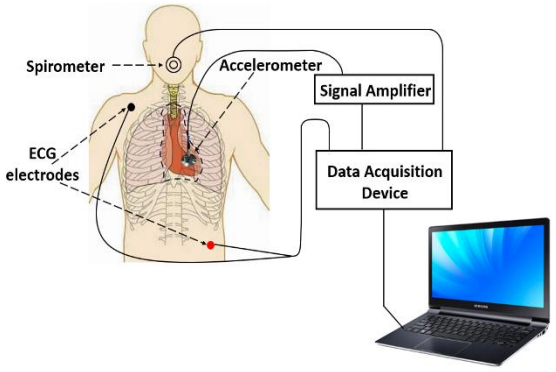

Figure 1. Experimental Setup

There is little published information about SCG variability during breath hold. This pilot study aims to quantify SCG variability during regular breathing in comparison with that at breath hold as during breath hold some of the factors causing variability (such as intrathoracic pressure) are almost constant.

II. MEASUREMENT OF THE SIGNALS

After IRB approval, 5 healthy male subjects with no known medical history of cardiovascular disease were

recruited for the study. Subject's demographics are listed in table 1.

Table 1. Subjects information

Age (years)	27.6±3.6
Height (Inches)	65.8±2.7
Weight (lbs.)	140.4±8.6
BMI	23.1±2.3

Subjects were asked to fast from food, caffeinated drinks and avoid strenuous exercise for at least 4 hours prior to the study to help exclude potential effects of exercise and eating on physiological processes affecting SCG. The experimental setup is shown in Figure 1.

Respiration flow was acquired by a spirometer (Model: SP-304, iWorx Systems, Inc., Dover, NH). The ECG signal was acquired by IX-B3G biopotential recorder (iWorx Systems, Inc., Dover, NH). Seismocardiographic signals were acquired using a tri-axial accelerometer (Model: 356A32, PCB Piezotronics, Depew, NY) which was affixed on the chest surface using double-sided medical grade tape at the 4th intercostal space near the left lower sternal border. The accelerometer measured acceleration in the dorsoventral, lateral and craniocaudal directions. The current study focusses on the dorsoventral-component of the acceleration (perpendicular to the chest wall). The SCG signal was amplified using a signal conditioner (Model: 482C, PCB Piezotronics, Depew, NY) with a gain of 100-fold.

Subjects were asked to rest on a 45-degree inclined bed head up position with their feet extended horizontally. Data was collected continuously for 3 minutes of regular breathing followed by 20~30 seconds of breath hold after end inspiration, then 30 seconds of regular breathing and then 20~30 seconds of breath hold after end expiration. During breath holding effort was made to maintain atmospheric intrapulmonary pressure by keeping the mouth and glottis open. A sampling frequency of 10 kHz was used for data acquisition. The acquired data was analyzed using Matlab (Matlab 2013, Mathworks, Natick, MA).

III. Signal Analysis

A. Filtering

Previous studies [5], [7], [16] suggested that the frequency content of SCG wave ranges from 0.5 Hz ~ 50 Hz. Hence the SCG and ECG signals were forward-backward filtered using a 4th order Chebyshev 2 type band-pass filter with a cut off 0.5-50 Hz with a stopband attenuation of 15 dB to reduce background noise (electronic noise~ 60 Hz) and baseline wondering due to respiration (<0.5 Hz). In addition, a moving average filter of order 5 was employed to further smooth the signal.

B. SCG events segmentation

The SCG signal was segmented into SCG events (also called heartbeats) using the R peaks of the ECG signal, which were detected using Pan Tomkins algorithm [17]. Each SCG event was selected to start 0.1 seconds before the R peak of the corresponding ECG and ends at 0.1 seconds before the next R peak.

C. Clustering SCG events

After segmentation, the SCG events were down sampled to 1000 Hz and were clustered based on their morphology using unsupervised machine learning. As the morphology of a SCG event may be best described by the signal amplitudes (at each data point of the event), amplitude values of SCG events were used as the feature vector input to the clustering algorithm. Here, k-medoid clustering was employed with dynamic time warping (DTW) as a dissimilarity measure. This clustering strategy has shown higher accuracies over other methods for shape-based (i.e., morphology-based) clustering of time series[18].

DTW is often used in time series clustering[18] due to its ability to deliver a more accurate dissimilarity measure of the signal morphologies determining the optimal "global alignment" between two time sequences by exploiting the temporal distortions between them [19]. In contrast, commonly used Euclidean distance may deliver suboptimal results when the time sequences are not aligned in time even if they have similar morphologies. A representation of the differences between DTW and

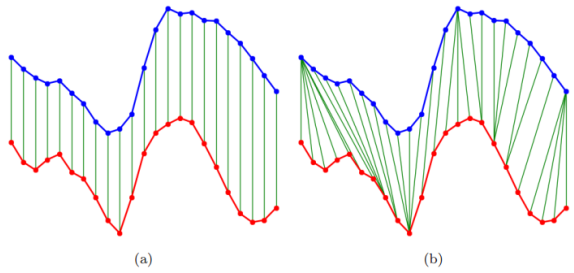

Figure 2. Associated points between two time series when the dissimilarity is measured with (a) Euclidean and (b) DTW measures.

Euclidean distance is shown in Figure 2 [20]. As SCG events are nonlinearly stretched due to heart rate variability, high variations in heart rate between different SCG events can cause significant mis-alignments, which would lead to discrepancies in the clustering results if Euclidean distance is used as a dissimilarity measure.

The clustering algorithm was implemented in MATLAB and is shown below.

Algorithm:

Inputs: Number of clusters= K. Set of SCG events: $\{X_1, X_2, X_3, \dots, X_i \dots, X_N\}$ where each event is defined by its feature vector (amplitude) as $X_i = \{x_1, x_2, x_3, \dots, x_{l_i}\}$. N is the number of events

Step 1: Initialize $C_1, \dots, C_j, \dots C_k$ as the medoids

Step 2: For each X_i find the nearest C_j and assign X_i to cluster j using DTW as the distance measure

Step 3: Update C_j based on the clustered events from previous step using equation 1.

$$C_j = argmin_{y \in \{X_{1j}, X_{2j}, \dots, X_{ij}, \dots, X_{nj}\}} \sum_{i=1}^{n_j} dtw(y, X_{ij}) \quad (1)$$

where, X_{ij} is the i^{th} event belongs to cluster j and n_j is the number of events belong to j after step 2.

Step 4: repeat step 2 and 3 till none of the cluster assignments change.

The time complexity of DTW is $\Theta(l^2)$, where l is the length of the SCG event [21]. To reduce the time complexity (and the computational time) of clustering in the current study, SCG events were down sampled to 1000 Hz. Prior to clustering, SCG events were normalized by their maximum amplitudes, which is not expected to affect DTW measure.

The elbow method was used to determine the optimum number of clusters by determining the fewest number of clusters that optimizes intra-cluster variance[15]. The intra-cluster variability was measured using equation 2, which calculates the average sum of distances (SOD) from each event to its cluster medoid. Here, X_{ij} is the i^{th} events belonging to cluster medoid C_j and n_j is the number of events belong to C_j. N is the total number of events used in the clustering.

$$SOD = \frac{1}{N} \sum_{j=1}^{k} \sum_{i=1}^{n_j} dtw(C_j, X_{ij}) \quad (2)$$

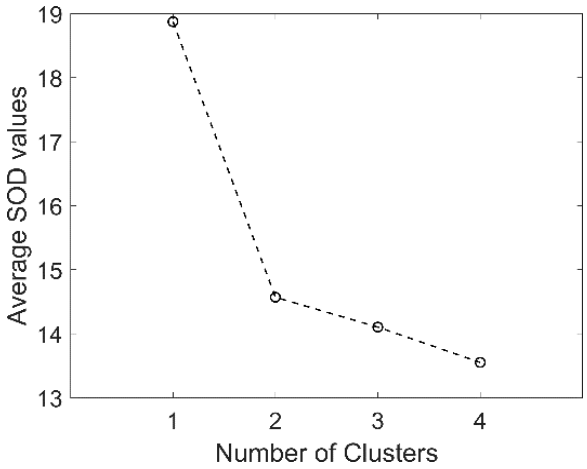

Figure 3. Average SOD for different number of clusters.

As shown in Figure 3, an elbow shape was observed when the number of clusters was 2, suggesting that 2 clusters would lead to optimal intra-cluster variance with fewest number of clusters. Previous studies on clustering SCG events during the breathing cycle have chosen same number of clusters [15].

IV. Results and Disscussion

To describe the clustering distribution during respiration, the timing of the clustered SCG events (as described by the time of their respective R peaks) was plotted on in Fig 4 in relation to the respiratory flow rate and lung volume (i.e. integral of the flowrate, see Figure 4).

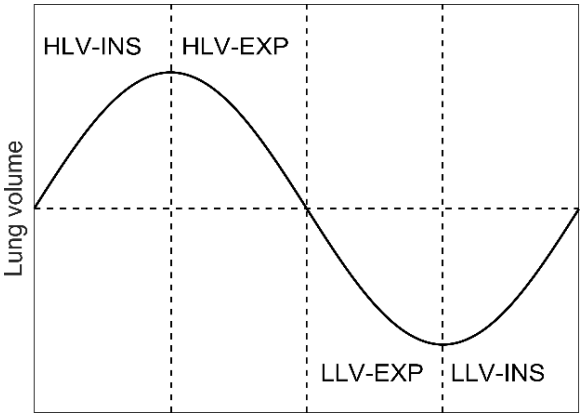

Figure 4. The four respiratory phases labeled in a simplified lung volume waveform Here, INSP, EXP, HLV and LLV denote inspiration, expiration, high lung volume and low lung volume, respectively.

Here, four respiratory phases are shown in Figure 4, where INSP, EXP, HLV and LLV denote inspiration, expiration, high lung volume and low lung volume, respectively.

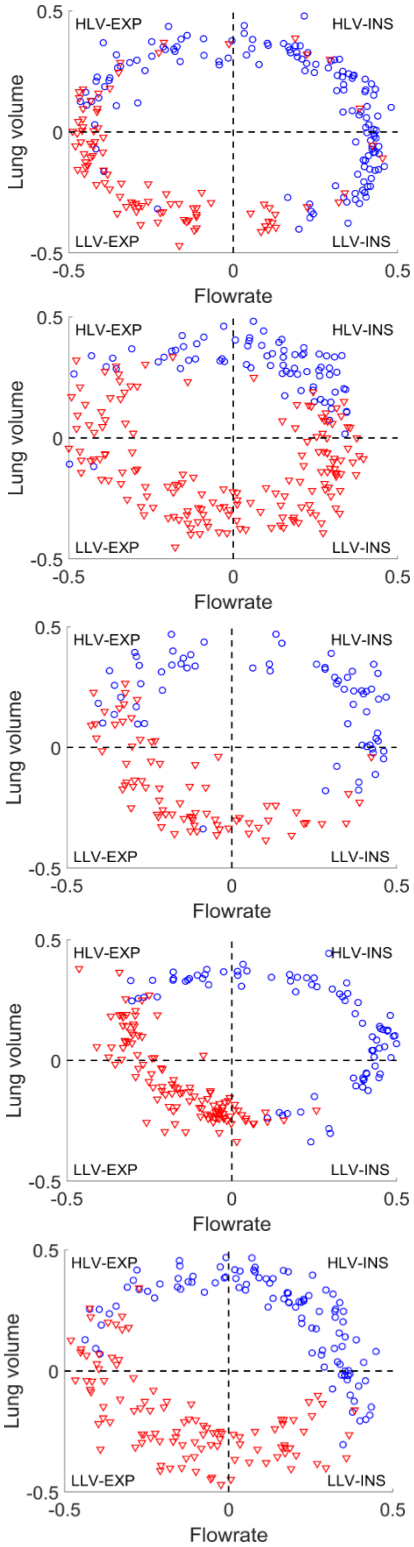

Figure 5 Cluster distribution in lung volume and flowrate space for all subjects. The blue circle represents cluster 1 while red triangles shows cluster 2 locations. The lung volume and flow rate axes were normalized to have a range of unity.

Figure 5 shows the cluster distribution on these four respiratory phases where SCG events belongs to cluster 1 and cluster 2 are labeled as blue 'o' circles and red '∇'triangles, respectively. These cluster distribution results showed that clusters are not separated entirely based on respiratory flow rate (i.e. by phase of inspiration vs expiration) or by lung volume. The regions HLV-INS and LLV-EXP were well separated compared to HLV-EXP and LLV-INS which showed more mixed clustering distributions. A recent study showed similar clustering patterns during normal breathing[15].

The cluster pattern was consistent in all study subjects and may be caused by changes in intrathoracic pressure, heart position (i.e. relative location of SCG sensor and heart), heart rate, or movements of the chest wall and diaphragm during breathing.

Acquiring SCG during different breath hold may help elucidate possible factors affecting SCG morphology. This may be possible since there are much smaller variations in intrathoracic pressure, heart position and chest wall movement during breath hold compared to during normal breathing. Therefore, SCG was acquired at two different breath hold states, namely, end inspiration and end expiration, which correspond to low and high intrathoracic pressures, respectively. Here, subjects were asked to breath regularly without taking deep breaths then perform breath hold with glottis open at end inspiration or end expiration. This was done to maintain intrathoracic pressures differences that are comparable to those of normal breathing. The acquired SCG morphology during breath hold were compared with that of normal breathing before and after clustering. The following section discusses this comparison in detail.

To quantify how two waveform groups are dissimilar, the intra and inter-group DTW distance were used. The following equations were used to calculate the intra and inter-group DTW distances.

$$Intra\text{—}group\ DTW = \frac{1}{n_1+n_2}\left[\sum_{i=1}^{n_1} dtw(C_1, X_{i1}) + \sum_{i=1}^{n_2} dtw(C_2, X_{i2})\right] \quad (3)$$

$$Inter\text{—}group\ DTW = \frac{1}{n_1+n_2}\left[\sum_{i=1}^{n_1} dtw(C_1, X_{i2}) + \sum_{i=1}^{n_2} dtw(C_2, X_{i1})\right] \quad (4)$$

Here, X_{i1}, X_{i2} are the i^{th} SCG event belonging to group 1 and group 2, respectively while C_1 and C_2 are the respective cluster medoids. And n_1, n_2 are the total number of events belong to group 1 and 2, respectively. Well separated groups are expected to have relatively low

intra-group DTW distance and high inter-group DTW distance.

The intra and inter-group DTW distances for normal breathing and breath hold are shown in Figure 6.

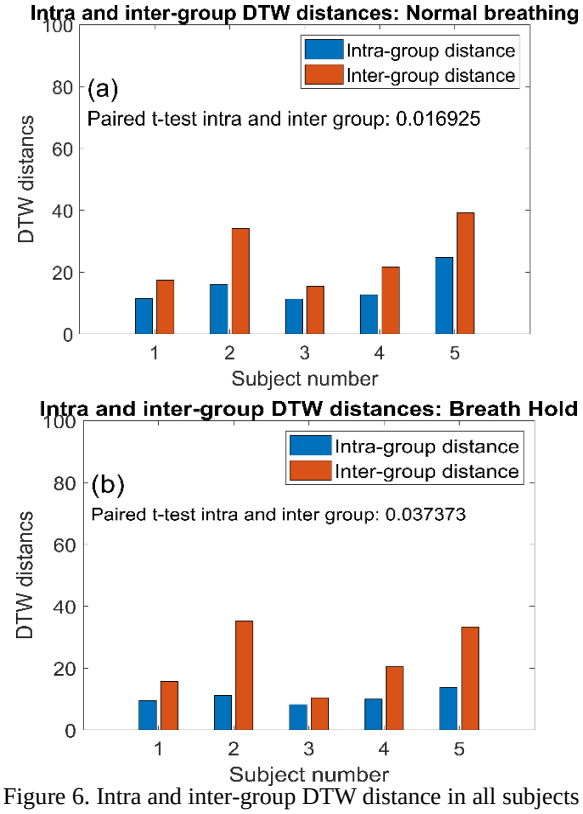

Figure 6. Intra and inter-group DTW distance in all subjects for (a) the two clusters obtained from SCG during normal breathing. (b) end inspiration vs end expiration during breath hold. The blue bars in the bottom figure are lower than those in the top figure suggesting that SCG had smaller variability during breath hold.

The top graph shows that distance for the two clusters identified from the normal breathing data. The bottom graph shows the distance for another two SCG groups, namely, the end expiration and end inspiration during breath hold.

Figure 6 suggests that the intra-group DTW distances for the breath hold groups are significantly smaller than those for normal breathing, which implies that SCG during breath hold has less variability. This result may be due to the less variation of intrathoracic pressure and heart location during breath hold. In addition, the inter-group variability was higher than intra-group distance, suggesting appropriate separation between groups for both Figure 6(a) and (b).

Furthermore, the inter-group DTW distance between normal breathing clusters and breath hold SCG were compared and shown in Figure 7.

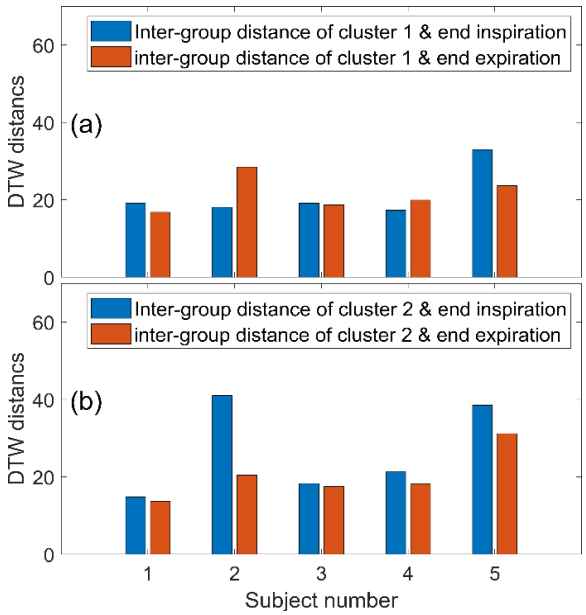

Figure 7. Inter-group DTW distance for end inspiration and expiration breath hold and (a) Cluster 1 and (b) Cluster 2. Cluster 1 and 2 were extracted from the normal breathing data using machine learning. This data suggests that Cluster 2 tended to be more similar to end expiration, while no clear trend was seen for Cluster 1.

Figure 7 shows that the inter-group distance between breath hold at end inspiration and expiration on one hand and (a) cluster 1 and (b) cluster 2 on the other hand. Figure 7 (b) shows that cluster 2 tended to have smaller distance to end expiration than end inspiration. This result is consistent with the fact that cluster 2 (see Figure 4) occurs at LLV which includes end expiration. Figure 7 (a) suggests that cluster 1 may be closer to either end inspiration or expiration breath hold. This may be because consistent control of end inspiration is harder (than end expiration) since it involves effort by the diaphragm and chest muscles that may not be consistently reproducible.

To investigate the SCG intra-group variability, intra-group distances were calculated under breath hold conditions and for normal breathing before and after clustering. These results are shown in Figure 8.

Figure 8 suggested that the average intra-group variability reduced significantly by 19% ($P<0.05$) after clustering and by 42% ($P<0.05$) during breath hold. This decrease in variability suggests possible utility for SCG measurements under breath hold conditions. A recent study[22] reported similar decrease in intra-group variability for normal breathing. It is to be noted that for critically ill patients, breath hold conditions are difficult

to produce for extended period of time. However, several short recordings of breath hold may be possible. Those

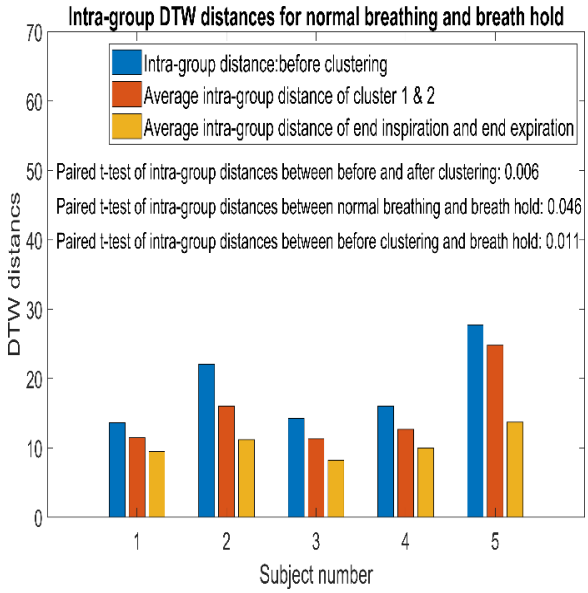

Figure 8. Intra-group DTW distances before and after clustering and under breath hold conditions.

can be patched to extract sufficient number of SCG events to perform signal analysis.

V. Summary

This study investigated SCG signal variability during normal breathing and breath hold. The SCG acquired during normal breathing were optimally clustered using unsupervised machine learning to reduce SCG morphological variability. The clustering results suggested that SCG waveforms were optimally separated into two groups that showed consistent relations with respiratory phases. The two breath hold states (end inspiration and expiration), which correspond to different physiological conditions (e.g., relative heart location shape and position, intra thoracic pressure) were found to have different SCG wave morphologies.

Intra-group SCG variability were compared for the un-clustered, clustered, and breath hold cases. Results showed that the variability was reduced by 19% after clustering and 42% during breath hold. Further studies in a larger number of subjects will help elucidate these differences in healthy subjects, and in those with cardiac pathologies.

Acknowledgments

This study was supported by NIH R44HL099053.

Hansen A Mansy and Richard H Sandler are part owners of Biomedical Acoustics Research Company, which is the primary recipient of the above grant, as such they may benefit financially as a result of the outcomes of the research work reported in this publication.

Reference

[1] B. S. Bozhenko, “Seismocardiography--a new method in the study of functional conditions of the heart,” *Ter. Arkh.*, vol. 33, p. 55, 1961.

[2] D. M. Salerno, “Seismocardiography: A new technique for recording cardiac vibrations. concept, method, and initial observations,” *J. Cardiovasc. Technol.*, vol. 9, no. 2, pp. 111–118, 1990.

[3] R. S. Crow, P. Hannan, D. Jacobs, L. Hedquist, and D. M. Salerno, “Relationship between seismocardiogram and echocardiogram for events in the cardiac cycle,” *Am. J. noninvasive Cardiol.*, vol. 8, pp. 39–46, 1994.

[4] K. Tavakolian *et al.*, “Myocardial contractility: A seismocardiography approach,” in *Engineering in Medicine and Biology Society (EMBC), 2012 Annual International Conference of the IEEE*, 2012, pp. 3801–3804.

[5] A. Taebi, “Characterization, Classification, and Genesis of Seismocardiographic Signals,” University of Central Florida, 2018.

[6] A. Taebi, R. H. Sandler, B. Kakavand, and H. A. Mansy, “Seismocardiographic Signal Timing with Myocardial Strain,” in *Signal Processing in Medicine and Biology Symposium (SPMB), 2017 IEEE*, 2017, pp. 1–2.

[7] A. Taebi and H. A. Mansy, “Time-Frequency Distribution of Seismocardiographic Signals: A Comparative Study,” *Bioengineering*, vol. 4, no. 2, p. 32, 2017.

[8] A. Taebi, A. J. Bomar, R. H. Sandler, and H. A. Mansy, “Heart Rate Monitoring During Different Lung Volume Phases Using Seismocardiography,” in *SoutheastCon 2018, IEEE*, 2018, pp. 1–5.

[9] A. Taebi and H. A. Mansy, “Grouping Similar Seismocardiographic Signals Using Respiratory Information,” in *Signal Processing in Medicine and Biology Symposium (SPMB), 2017 IEEE*, 2017, pp. 1–6.

[10] G. Shafiq, S. Tatinati, W. T. Ang, and K. C. Veluvolu, “Automatic identification of systolic time intervals in seismocardiogram,” *Sci. Rep.*, vol. 6, p. 37524, 2016.

[11] M. K. Azad, P. T. Gamage, and R. H. Sandler, “Detection of respiratory phase and rate from chest surface measurements,” *J Appl Biotechnol Bioeng*, vol. 5, no. 6, pp. 359–362, 2018.

[12] V. Zakeri, A. Akhbardeh, N. Alamdari, R. Fazel-Rezai, M. Paukkunen, and K. Tavakolian, “Analyzing Seismocardiogram Cycles to Identify the Respiratory Phases,” *IEEE Trans. Biomed. Eng.*, vol. 64, no. 8, pp. 1786–1792, 2017.

[13] K. Pandia, O. T. Inan, G. T. A. Kovacs, and L. Giovangrandi, “Extracting respiratory information from seismocardiogram signals acquired on the chest using a miniature accelerometer,” *Physiol. Meas.*, vol. 33, no. 10, p. 1643, 2012.

[14] B. E. Solar, A. Taebi, and H. A. Mansy, “Classification of Seismocardiographic Cycles into Lung Volume Phases,” in *Signal Processing in Medicine and Biology Symposium (SPMB), 2017 IEEE*, 2017, pp. 1–2.

[15] P. T. Gamage, M. Khurshidul.Azad, A. Taebi, R. H. Sandler, and H. A. Mansy, “Clustering Seismocardiographic Events using Unsupervised Machine Learning,” in *2018 IEEE Signal*

Processing in Medicine and Biology Symposium (SPMB), 2018, pp. 1–5.

[16] K. Pandia, O. T. Inan, and G. T. A. Kovacs, "A frequency domain analysis of respiratory variations in the seismocardiogram signal," in *2013 35th Annual International Conference of the IEEE Engineering in Medicine and Biology Society (EMBC)*, 2013, pp. 6881–6884.

[17] J. Pan and W. J. Tompkins, "A real-time QRS detection algorithm," *IEEE Trans. Biomed. Eng*, vol. 32, no. 3, pp. 230–236, 1985.

[18] J. Paparrizos and L. Gravano, "Fast and accurate time-series clustering," *ACM Trans. Database Syst.*, vol. 42, no. 2, p. 8, 2017.

[19] H. Sakoe, S. Chiba, A. Waibel, and K. F. Lee, "Dynamic programming algorithm optimization for spoken word recognition," *Readings speech Recognit.*, vol. 159, p. 224, 1990.

[20] Z. Zhang, P. Tang, L. Huo, and Z. Zhou, "MODIS NDVI time series clustering under dynamic time warping," *Int. J. Wavelets, Multiresolution Inf. Process.*, vol. 12, no. 05, p. 1461011, 2014.

[21] F. Petitjean, G. Forestier, G. I. Webb, A. E. Nicholson, Y. Chen, and E. Keogh, "Dynamic time warping averaging of time series allows faster and more accurate classification," in *2014 IEEE international conference on data mining*, 2014, pp. 470–479.

[22] R. H. Sandler *et al.*, "Minimizing Seismocardiography Variability by Accounting for Respiratory Effects," *J. Card. Fail.*, vol. 25, no. 8, p. S172, 2019.